Nonlinear Dynamics **33:** 253–265, 2003.

Dynamics Analysis of Ground Contact Pressure of English Pointer Dogs

DAN B. MARGHITU
Department of Mechanical Engineering, Auburn University, 202 Ross Hall, Auburn, AL 36849, U.S.A.

STEVEN F. SWAIM
Scott Ritchey Research Center, Auburn University, AL 36849, U.S.A.

PAUL F. RUMPH
Department of Anatomy, Auburn University, AL 36849, U.S.A.

DORIAN COJOCARU
Department of Automation, University of Craiova, Romania

ROBERT L. GILLETTE
Sport Medicine Program, College of Veterinary Medicine, AL 36849, U.S.A.

M. STACIE SCARDINO
Scott Ritchey Research Center, Auburn University, AL 36849, U.S.A.

(Received: 28 January 2003; accepted: 4 August 2003)

Abstract. In this study force sensing resistors were used to determine the pressure on the central area of each of the weight bearing pads of the fore and hind paws of dogs at the walk. Six adult normal healthy English Pointer dogs were used in this project. Pressure data were collected by affixing a force sensing resistor to the central area of the ground contact surface of each weight bearing paw pad of the right fore and hind limbs. Pressure signal data from stance phase during walking were analyzed. Within paw pads, the pressure graphs were consistent in form and magnitude. Within paws, there were significant pressure differences among pads on both fore and hind limbs. The coefficient of restitution, the embedding dimension, and the Lyapunov exponents were calculated. The ability to measure and analyze pressure on individual paw pads provides insight into soft tissue stresses on the palmar/plantar surface of the paw. Pressure at a wound site on the pads has a detrimental effect on wound healing and a better understanding these stresses will be of benefit when suturing and bandaging pad wounds. Such information is especially important in athletic and working dogs, e.g. search and rescue dogs.

Keywords: Paw pad, ground reaction force, force sensing resistor, coefficient of restitution, embedding dimension.

1. Introduction

The foot pads (tori or pulvini) of dogs are hairless and heavily keratinized. There are functional pads on each of the four weight bearing digits, and a larger one on the central area of the distal metapodium. The pads contain sweat glands and some are partially or fully pigmented. The thickened cornified epithelium is supported by an underlying thick subcuticular bed (pad) of fatty connective tissue. The pad is designed to resist friction and cushion force (absorb shock). Paw pads are often injured and require protection during wound healing. Common lesions of the pads include ulcers, lacerations, dermatitis, denervation (trophic) ulcers, penetrating wounds, abrasions, chemical burns, thermal injury and work related partial epidermal sloughing ('blowing a pad'). Many of these conditions require suturing or application of band-

ages. Ground contact pressure on the pads is counter productive to healing as the pads spread with weight-bearing [1, 2]. This aggravates most lesions or tends to separate lacerations and promotes wound dehiscence.

Quantitative analysis of locomotion has become a valuable complement for basic and applied studies of sports performance and for diagnosis and treatment of orthopedic, muscular and neurological diseases. Technologies are now available to objectively measure various aspects of animal movements. Stationary force platforms positioned in the floor or under treadmills have been frequently used for gathering ground reaction force data. The platforms contain piezoelectric crystals or strain gauges and furnish data that reflect the total force at the foot/ground contact during the stance phase of the step cycle.

Ground reaction forces have been measured in dogs during normal and abnormal locomotion and they have been used to evaluate therapeutic strategies [3, 4]. Study of discrete palmar/plantar pressures in animals has largely been limited to placement of pressure transducers under shoes in horses [5].

To our knowledge, the use of kinetic and nonlinear dynamic analysis tools that provide information has not been reported in dogs and there is little information about the pressure on discrete areas of the paw pad surface.

The ability to measure pressure on individual paw pads would provide information about soft tissue stresses on the palmar/plantar surface of the paw. Pressure at a wound site has a detrimental effect on wound healing and a better understanding of these stresses will be of benefit when suturing and bandaging wounds. This information would be particularly useful in canine athletes and working dogs where pad injuries are common due to the nature of the dog's activity. Rapid healing is required for early return to those activities, e.g. search and rescue work.

To investigate the causes of discrete local injuries to the paw pads or evaluate the effect of bandaging techniques, it was necessary to know the pressure on pads. The objective of this study was to use force sensing resistors to determine the pressure on the central area of the digital and metacarpal pads of the fore limb as well as the digital and metatarsal pads of the hind limb on 6 clinically normal English Pointer dogs at the walk. Based on the pressure information the coefficients of restitution were computed to study the dynamic interaction of the pad and ground surface. The nonlinear analysis tools were applied for the measured pressure.

2. Materials and Methods

Six English Pointer dogs of either sex and weighing from 13.4 to 21.8 kg were selected as a representative of working dogs subject to typical paw pad lesions. The study was conducted under protocols approved by the Auburn University Institutional Animal Care and Use Committee. The dogs were given physical and hematologic examinations and were treated for external and internal parasites. Additionally, each dog received an orthopedic examination of all limbs. The dogs underwent a period of habituation consisting of familiarization with the handler, laboratory, walking with a booty and wire loosely taped to the limbs, and manipulation of the fore and hind paws. Pressure data were collected by affixing a force sensing resistor to the central area of the ground surface of each weight bearing paw pad of the right fore and hind limbs. Resistors were connected to a microcomputer by a stranded cable suspended by pulleys from a tension wire (Figure 1). Pressure signal data from stance phase during walking

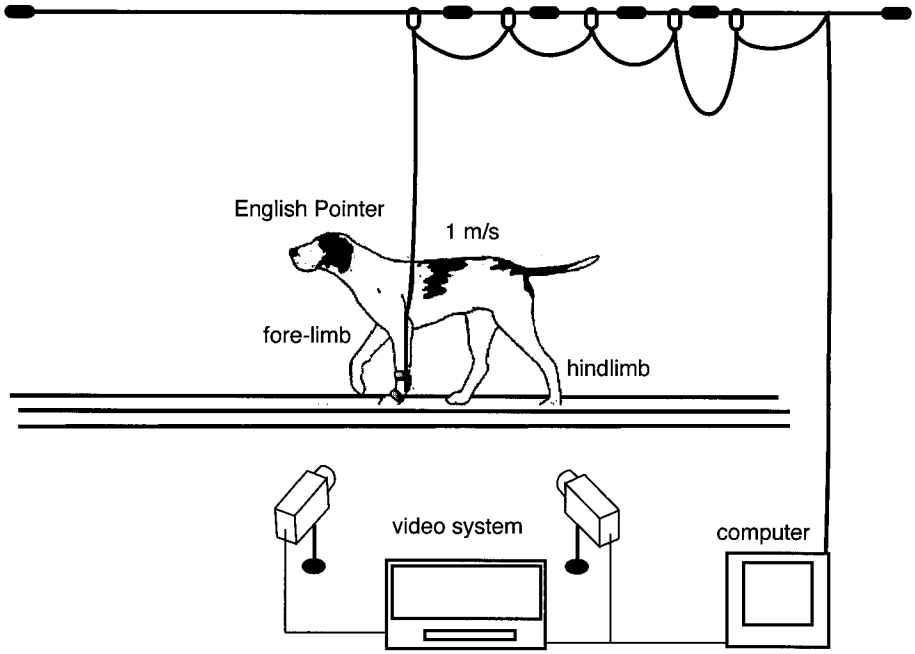

Figure 1. Experimental set-up.

were analyzed. The force sensing resistors are polymer thick film devices that respond to applied surface force by decreasing electrical resistance. Each force sensing resistor had an active radius of 5 mm (Figure 2).

Individual pressure calibration curves were established for each resistor before use and their function was checked against the curves after use. Each dog was lead at approximately 1 m/s in a straight line from end to end of the laboratory as data were collected at a rate of 400 Hz. The process was repeated for fore and hind limbs and the sessions were videotaped for later review. The dogs were well behaved and after habituation, patiently tolerated the application of sensors, connection to computer, and the data collection routine. The presence of sensors on the paws did not appear to alter their gait.

3. Coefficient of Restitution

The kinetic coefficient of restitution (Poisson) e is defined as the ratio of the impulse during restitution phase, P_r over the impulse during compression phase P_c

$$e = \frac{P_r}{P_c} = \frac{\int_{t_m}^{t_2} F_r \, \mathrm{d}t}{\int_{t_1}^{t_m} F_c \, \mathrm{d}t}, \tag{1}$$

where F_r is the normal contact force during restitution $[t_m, t_2]$ and F_c is the normal contact force during compression $[t_1, t_m]$. The time at which the paw and the ground first come into contact is t_1. Maximum compression time is t_m and the separation time is t_2.

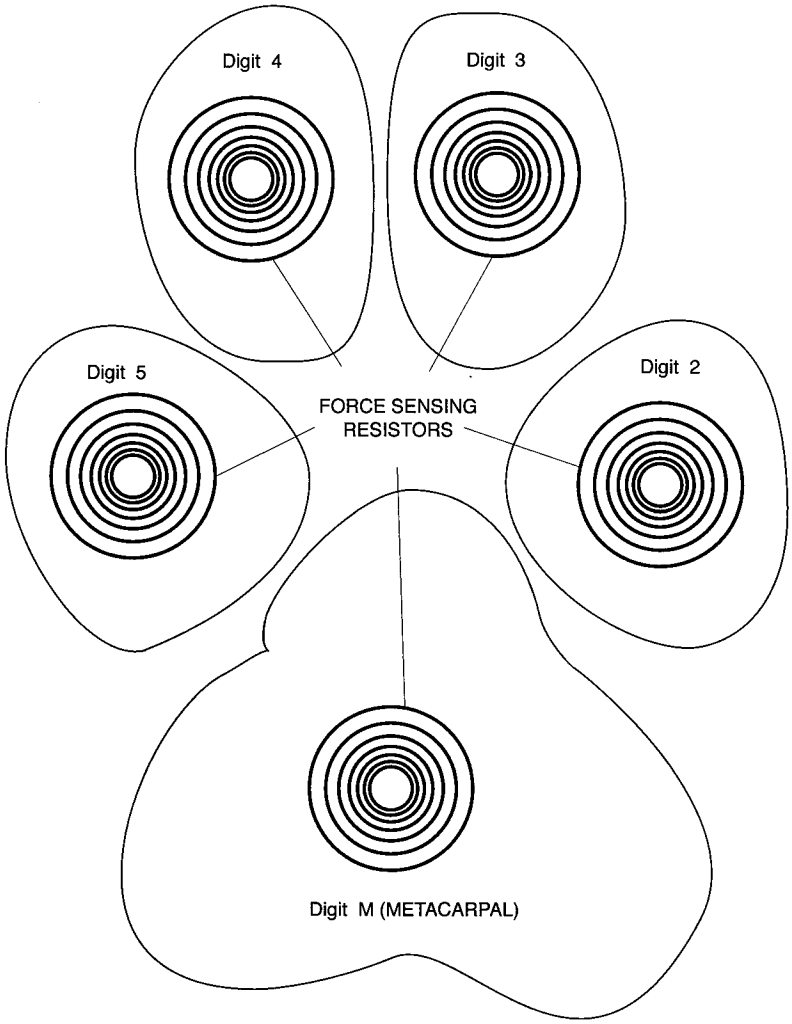

Figure 2. Force sensing resistors and the area of the paw pad.

Since the time integrals of the force are equal to areas in the graph corresponding to each phase of the collision, the coefficient of restitution will be

$$e = \frac{A_r}{A_c}, \tag{2}$$

where A_r and A_c are the restitution and compression areas, respectively. From the experimental data the areas A_r and A_c were calculated.

4. State Space Reconstruction

One method to reconstruct the state space S is to generate the so-called delay coordinates vectors [6]

$$\mathbf{x}_n = \{s(t_0 + n\tau_s), s(t_0 + n\tau_s + \tau), \ldots, s(t_0 + n\tau_s + (d_E - 1)\tau)\}, \tag{3}$$

where $s(\cdot)$ is a measured scalar function (contact pressure), τ_s the sampling time, $n = 1, 2, \ldots, d_E$, $\tau = k\tau_s$ an appropriately chosen time delay. The space constructed by using the vector x_n is called the reconstructed space. The integer d_E is called the embedding dimension.

The embedding dimension d_E must be large enough so that the reconstructed orbit does not overlap with itself. When this happens, d_E is called the proper embedding dimension. The dynamics in the reconstructed state space is equivalent to the original dynamics. As a consequence of the equivalence, an attractor in the reconstructed state space has the same invariants, such as Lyapunov exponents and dimension [7].

5. Correlation Dimension

There are various ways to define the dimension of an attractor, which is generally fractional. One of them is the correlation dimension d_L. The definition of the correlation dimension is extracted from the correlation integral

$$C_2(l) = \lim_{N\to\infty} (1/N^2) \sum_{i=1}^{N} \sum_{i,j=1}^{N} H(l - |\mathbf{x}_i - \mathbf{x}_j|),$$

where N is the number of points in a set, $\mathbf{x}_i - \mathbf{x}_j$ is the vector separating the ith and jth points, H is the Heaviside function, l is the radius of a sphere constructed around each point $\mathbf{x}_i$ in the state space. The correlation integral is obtained by counting the number of points within the sphere. As l approaches zero, it is expected that the correlation integral have the form

$$C_2(l) \simeq l^{d_L},$$

where d_L is called the correlation dimension.

Grassberger and Procaccia stated that

$$d_L < F,$$

where F denotes the number of degrees of freedom of the system.

6. False Nearest Neighbors

It is necessary to determine an appropriate embedding dimensions of the state space in which the state trajectories do not overlap. To find a proper embedding dimension d_E, the false nearest neighbors method (FNN) or global false nearest neighbors method can be applied [8]. The global false nearest neighbors analysis compares the distances between neighboring trajectories at successively higher dimension. 'False neighbors' occur when trajectories that overlap in embedding dimension d_i are distinguished in embedding dimension d_{i+1}. As i increases, the total percentage of false neighbors (%FN) declines and d_E is chosen where this percentage approaches zero.

The embedding dimension d_E is useful for the determination of the local false nearest neighbors. One can inquire about the local structure of the phase space to see if locally one requires fewer dimension than d_E to capture the evolution of the orbits as they move on the attractor.

Working in a determinated space one can move to a point $\mathbf{x}(k)$ on the attractor and one can find a subspace of dimension $d_L \leq d_E$ that makes accurate local neighborhood to neighborhood maps of the data on the attractor. One can define a neighborhood by specifying

the number of neighbors N_B for the point $\mathbf{x}(k)$ and then can provide a local rule for how these points evolve in one time step into the same N_B points near $\mathbf{x}(k+1)$. One can test the quality of these predictions (P_k) and can seek a value of d_L where the quality of these predictions become independent of d_L and of the number of neighbors N_B. If one can choose the eigendirection associated with largest d_L eigenvalue of the covariant matrix, one can find the best local dynamical dimension d_L [8]. The determination of the local dimension d_L of the dynamics by the local false nearest neighbor method shows how many dimensions one can use to model the dynamics. The local dimension also shows how many true Lyapunov exponents one should evaluate for the system. When the percentage of bad predictions (P_k) becomes independent of d_L and is also insensitive to the number of neighbors N_B, one may say that we have identified the correct local dimension for the active dynamical degrees of freedom. This is the local criterion for the dynamical degrees of freedom.

7. Lyapunov Exponents

Lyapunov exponents provide a measure of the sensitivity of the system to its initial conditions [9]. They exhibit the rate of divergence or convergence of the nearby trajectories from each other in state space and are fundamentally used to distinguish the chaotic and non-chaotic (periodic or quasi-periodic) behavior. Periodic attractors show only negative and zero exponents which indicate convergence to a predictable motion, whereas there exists at least one positive exponent for a chaotic system. Therefore, one needs to determine the sign of Lyapunov exponents to characterize the behavior of a dynamically system. If one considers a three-dimensional state space, so that there will be an exponent for each dimension: all negative exponents will indicate the presence of a fixed point; one zero and the other negative a limit cycle; one positive a chaotic attractor.

The magnitudes of Lyapunov exponents quantify dynamics in information theoretic terms. The exponent measures the rate at which system processes create or destroy information. Thus, the exponents are expressed in bits of information/s.

8. Results

Data from stance phase during walking were analyzed. Mean pressures and coefficients of restitution were compared among dogs and digits.

The similarities and general characteristics of form and magnitude of contact pressure between fore and hind limb are demonstrated in composite graphic representations of pad pressure during contiguous step cycles (Figures 3 and 4). Within dogs, the general patterns of pressure were studied from pressure/time sequences assembled for each digit (Figures 5 and 6). The signals from the stance phase of all pads had a single peak.

Each pad had a consistent and distinctive slope for the compression and restitution phases of the step cycle. During the walking, the peak pressures among pads occurred at slightly different times in the stance phase.

For every pad, the mean peak pressures did not differ significantly among dogs. From subjective evaluation of these graphs, it was evident that pressures on each pad were consistent among steps but there appeared to be substantial differences among pads.

Within paws the greatest pressures were recorded from digits 3 and 5, and lesser pressures were recorded from digits 2 and 4. The metapodial pad pressures were intermediate between

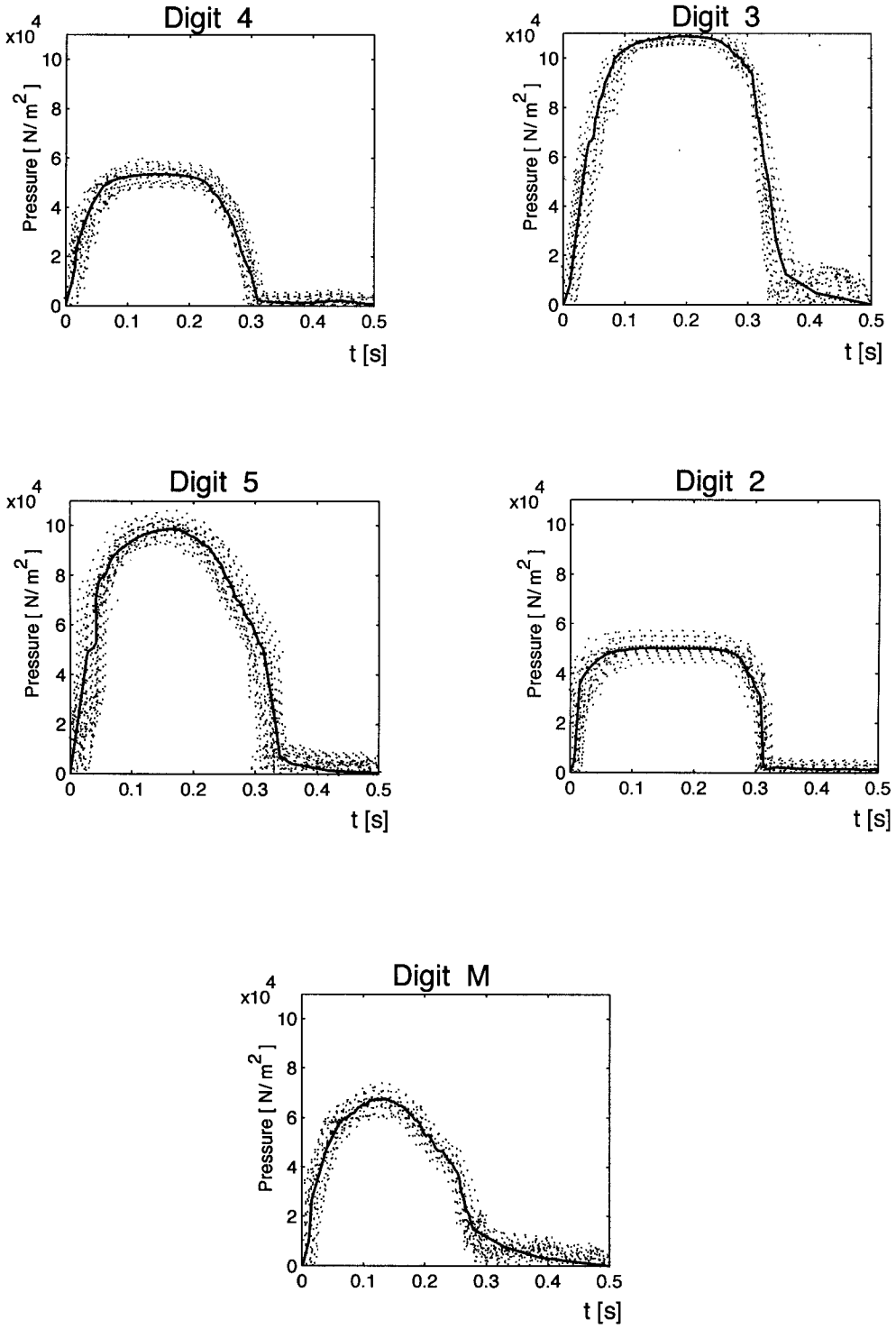

Figure 3. Pressure distribution for the fore limb.

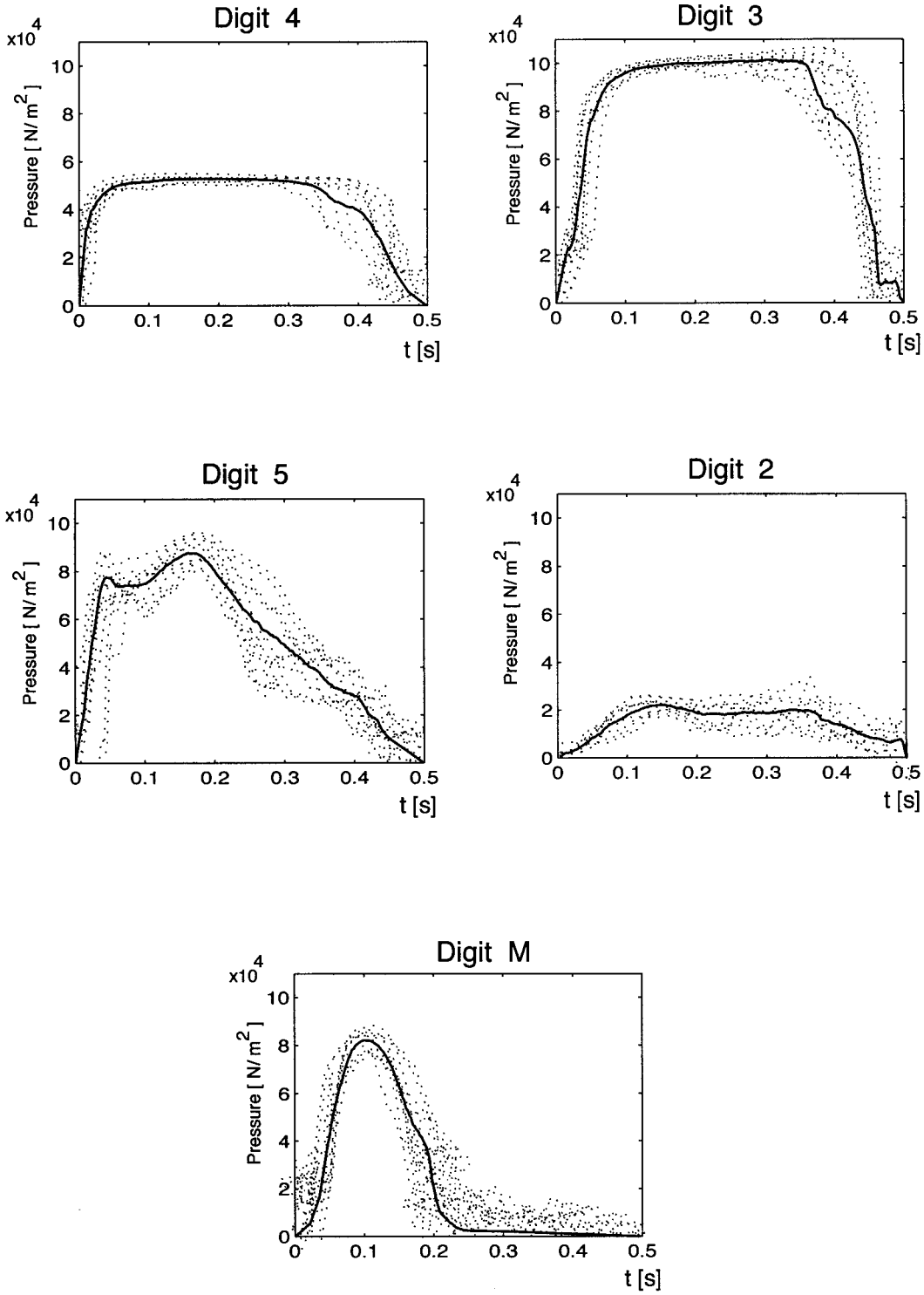

Figure 4. Pressure distribution for the hind limb.

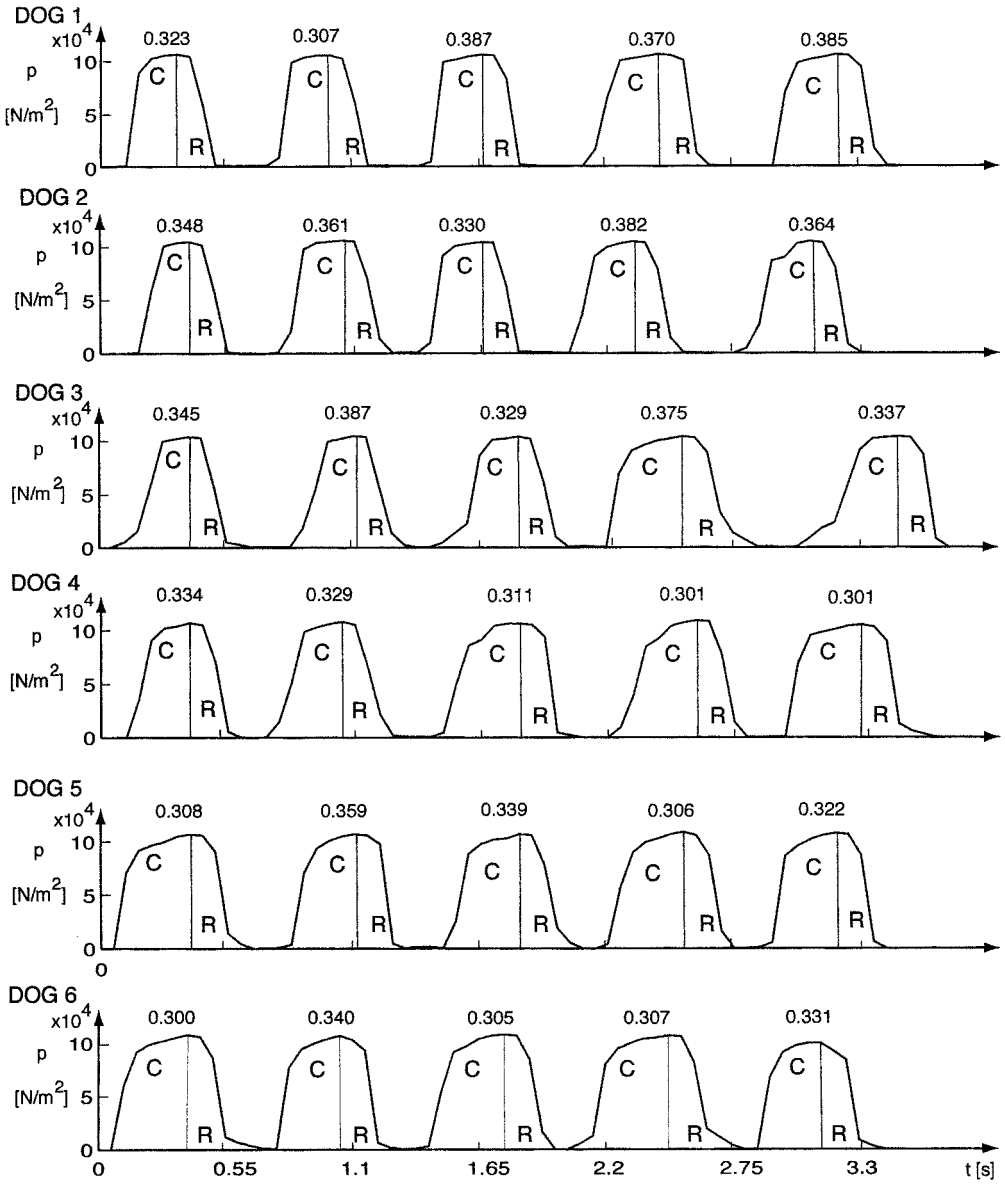

Figure 5. Coefficient of restitution for the digit 3 of the fore limb for 5 steps. C – compression phase, R – restitution phase.

these groups. The mean peak pressures among pads were significantly different and these findings were consistent for both fore and hind limb pads.

Coefficients of restitution reflected the energy loss (plasticity) at the pad/ground interface. As with peak pressures, the differences among dogs was not significant (Figure 7). Consistently, the metapodial pads were the least plastic. Among fore limb digits, the second and fourth were most plastic and were not significantly different. Mean coefficients of restitution from all pads of the hind limb were significantly different from one another. Digit 3 was the most plastic of hind limb pads.

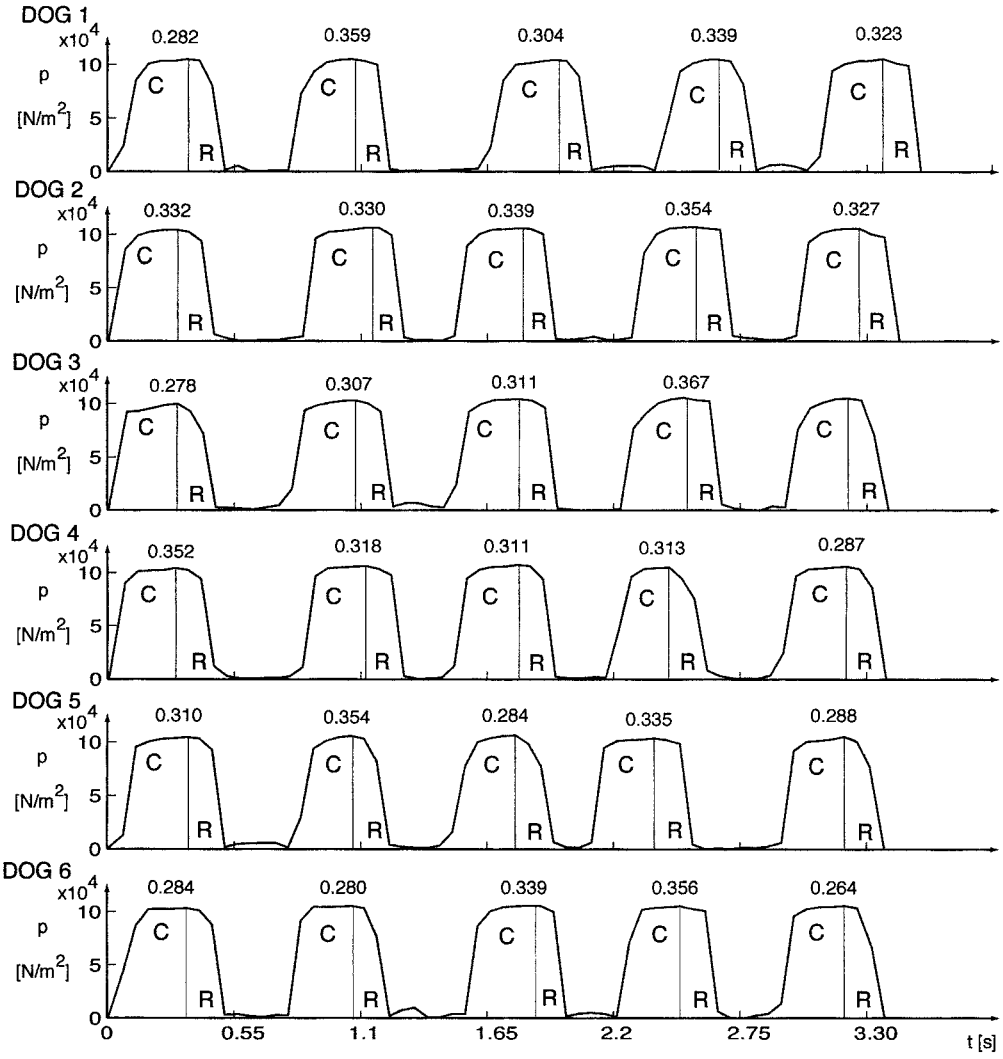

Figure 6. Coefficient of restitution for the digit 3 of the hind limb for 5 steps. C – compression phase, R – restitution phase.

For the contact pressure there is a sharp drop at the embeding dimension $d_E = 3$ after which the percentage of false nearest neighbors (%FN) remains constant (Figure 8). The data from the pressure showed that percentage of global false nearest neighbors (%FN) remain constant after $d_E = 3$. The same analysis were performed for al the digits.

The percentage of bad predictions P_k for pressure becomes independent of number of neighbors N_B at the local dimension $d_L = 3$, and where $d_L = 3$ represents the number of degrees of freedom of the system. One can conclude that the number of Lyapunov exponents is 3 and the system has 3 degrees of freedom.

The type of dynamical evolution is best shown by the sign of the largest Lyapunov exponent. We know that $d_E = d_L = 3$ from the earlier analysis of the system. Using $d_E = d_L = 3$ one can calculate the largest Lyapunov exponents. The largest Lyapunov exponents λ_1 for digit 3 are: $\lambda_1 \in [0.34,\ 0.87]$.

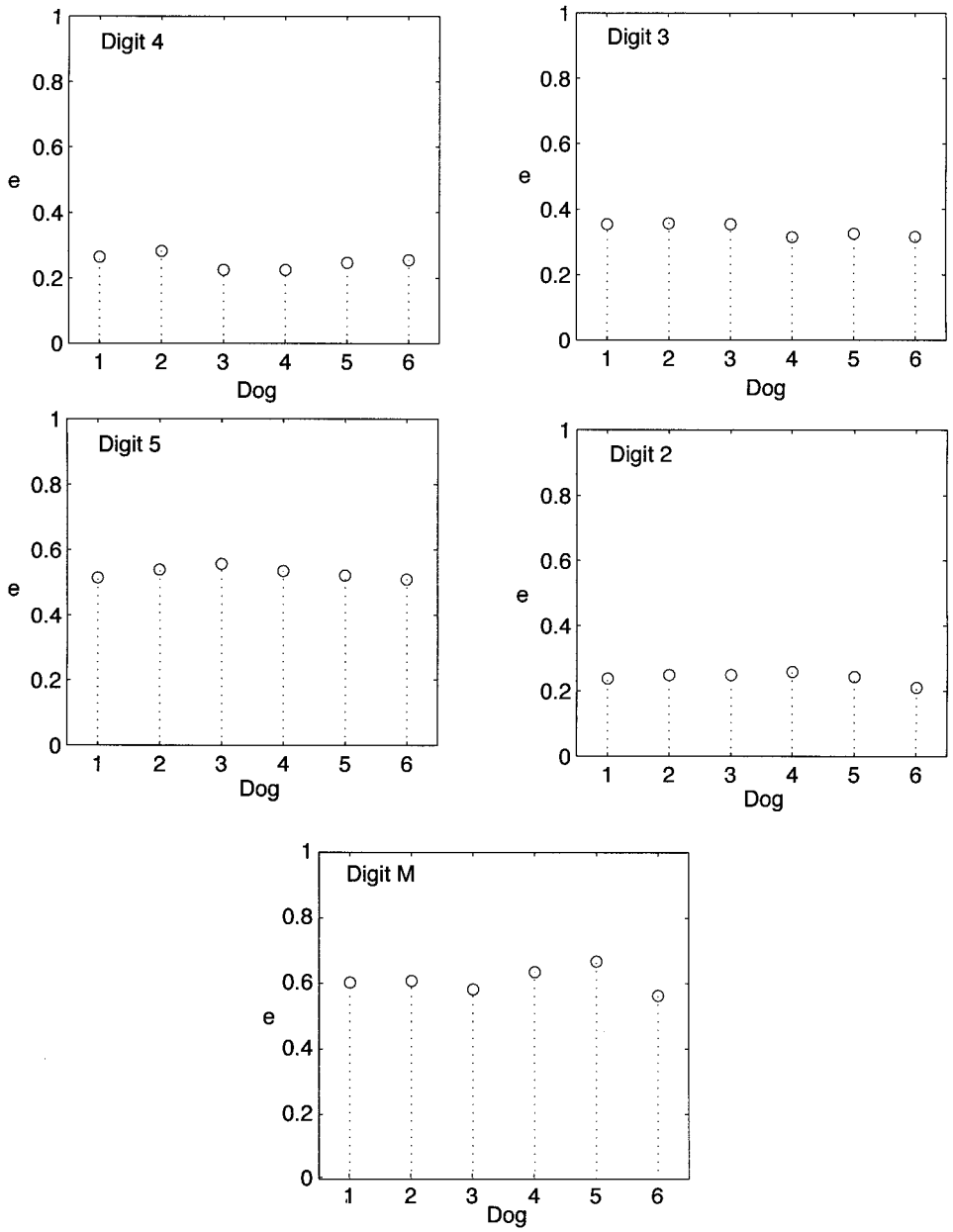

Figure 7. Global coefficient of restitution for the fore limb.

The sign of the largest Lyapunov exponent is positive for all data, denoting the exponential separation of nearby trajectories as time evolves, that is, a chaotic behavior. So, one can conclude at this point the chaotic behavior of the system.

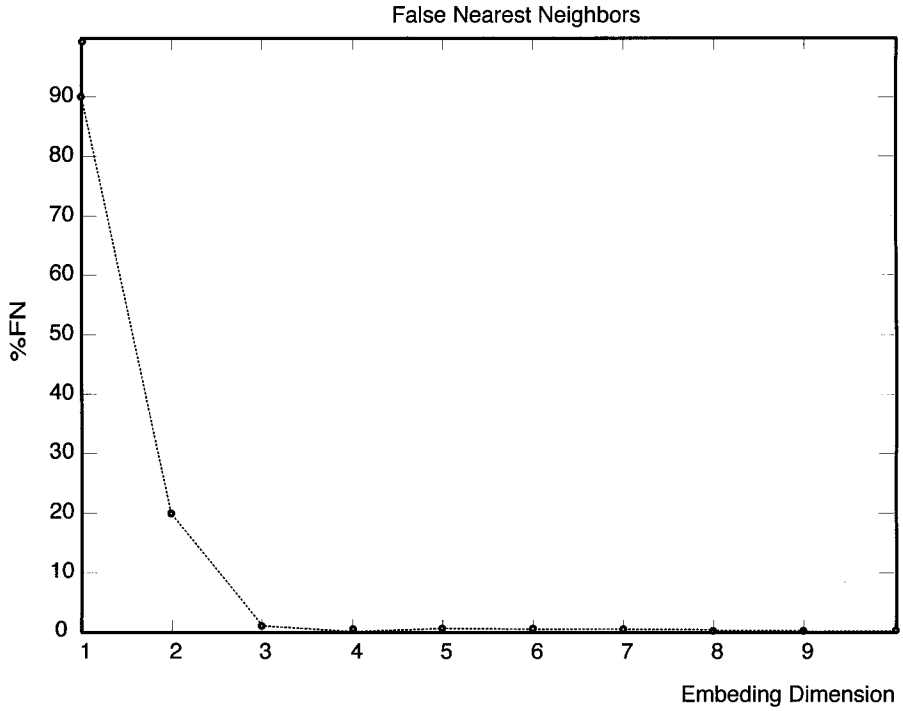

Figure 8. Embedding dimension for the digit 3 of the fore and hind limb.

9. Conclusion

Within paw pads, the pressures were very consistent in form and magnitude. Digital pads 3 and 5 had the greatest pressures while digital pads 2 and 4 had the least pressure. Metapodial pads had maximum pressures that were intermediate in magnitude for each paw.

Coefficients of restitution were calculated to study the dynamic interaction of the pad and ground surface. The significant differences among pads suggests that there were either differences in plastic nature of tissue components, anatomical structures or how individual pads compress and recover as the step cycle progresses. The metapodial pads were consistently the least plastic of the foot pads. The proper embedding dimension is three and the largest Lyapunov exponents are positive for all data.

The techniques reported here provide a method for evaluating bandaging techniques and materials, that can be used for alleviating pressure on the palmar/plantar paw surface of the canine paws to enhance the wound healing process.

References

1. Basher, A., 'Foot injuries in dogs and cats', *Compendium on Continuing Education Practicing Veterinarian* **1b**, 1994, 1159–1176.
2. Swaim, S. F., 'Management and bandaging of soft tissue injuries of dog and cat feet', *Journal of the American Animal Hospital Association* **21**, 1985, 329–340.
3. Budsberg, S. C., Verstraete, M. C., and Soutas-Little, R. W., 'Force plate analysis of the walking gait in healthy dogs', *American Journal of Veterinary Research* **48**, 1987, 915–918.
4. Roush, J. K. and McLaughlin, R. M., 'Effects of subject stance time and velocity on ground reaction forces in clinically normal Greyhounds at the walk', *American Journal of Veterinary Research* **55**, 1994, 1672-1676.

5. Ratzlaff, M. H., Hyde, M. L., and Grant, B. D., 'Measurement of vertical forces and temporal components of the strides of horses using instrumented shoes', *Equine Veterinary Science* **10**, 1990, 23–35.
6. Packard, N. H., Crutchfield, J. P., Farmer, J. D., and Shaw, R. S., 'Geometry from a time serie', *Physical Review Letters* **45**, 1980, 712–716.
7. Ott, E., Sauer, T., and Yorke, J. A., *Coping with Chaos*, Wiley, New York, 1994.
8. Abarbanel, H. D. I., *Analysis of Observed Chaotic Data*, Springer-Verlag, New York, 1996.
9. Nayfeh, A. H. and Balachandran, B., *Applied Nonlinear Dynamics*, Wiley, New York, 1995.